Heriot-Watt University
Research Gateway

Numerical studies of multiphase flow and separation performance of natural medium cyclones for recovering waste coal

Citation for published version:
Chu, K, Chen, J, Yu, A & Williams, RA 2017, 'Numerical studies of multiphase flow and separation performance of natural medium cyclones for recovering waste coal', *Powder Technology*, vol. 314, pp. 532-541. https://doi.org/10.1016/j.powtec.2016.10.047

Digital Object Identifier (DOI):
10.1016/j.powtec.2016.10.047

Link:
Link to publication record in Heriot-Watt Research Portal

Document Version:
Peer reviewed version

Published In:
Powder Technology

General rights
Copyright for the publications made accessible via Heriot-Watt Research Portal is retained by the author(s) and / or other copyright owners and it is a condition of accessing these publications that users recognise and abide by the legal requirements associated with these rights.

Take down policy
Heriot-Watt University has made every reasonable effort to ensure that the content in Heriot-Watt Research Portal complies with UK legislation. If you believe that the public display of this file breaches copyright please contact open.access@hw.ac.uk providing details, and we will remove access to the work immediately and investigate your claim.

Download date: 10. Oct. 2024

Numerical studies of multiphase flow and separation performance of natural medium cyclones for recovering waste coal

Kaiwei Chu[1*], Jiang Chen[1], Aibing Yu[1] and Richard A. Williams[2]

[1]*Laboratory for Simulation and Modelling of Particulate Systems, Department of Chemical Engineering, Monash University, Clayton, VIC 3800, Australia*

[2]*Heriot-Watt University, Edinburgh Campus, Edinburgh, Scotland, EH14 4AS*

**Corresponding author: Email: kevin.chu@monash.edu; Tel: +61399050848*

ABSTRACT

Coal has been a major energy resource worldwide for many years and will continue to be in the foreseeing future. One of the major by-products of using coal is the redundant colliery spoil heaps that are harmful to environments. This problem can be overcome in a relatively economical way by using a newly developed technology, i.e., the Nature Medium Cyclone (NMC) technology which makes use of fine dirty particles in the feed rather than magnetite particles to form the medium phase. The current understanding on the flow and performance of NMCs are extremely limited. In this work, the flow in a NMC is studied by using a combined approach of Computational Fluid Dynamics (CFD) and Discrete Element Method (DEM) (CFD-DEM) where the flow of coal particles is modelled by DEM and that of medium flow by conventional CFD. The simulated results are compared favourably with physical experiments and the effects of two of the most important operational parameters, i.e., medium velocity and medium-to-coal ratio (M:C ratio) at the NMC inlet, are investigated numerically.

Keywords: Multiphase flow; Nature Medium Cyclone; Discrete Element Method; Computational Fluid Dynamics; Physical separation.

1 INTRODUCTION

A major by-product in coal production is the redundant colliery spoil heaps that are harmful to environments since they may cause contamination (e.g., spontaneous combustion of coal within the spoil and pollution of surface and ground waters) from within the existing spoil tip. This problem can be overcome by using a newly developed technology, i.e., the Nature Medium Cyclone (NMC) technology that is currently unique to recover waste coal from redundant colliery spoil heaps or abandoned coal reserve sites. It is an environment-friendly coal recovery and restoration technology since it eliminates environmental hazards and the site after treatment could be used as landscape (e.g., public open space for biodiversity enhancement and recreation).

Table 1 compares the NMC technology with the popular coal-upgrading technology of large coal particles, i.e., the Dense Medium Cyclone (DMC) technology. It can be seen that the most important advantage of the NMC technology is that it does not use an additive such as magnetite in the liquid circuit to form medium density. Instead, it uses the fine dirt, shale and clay within the feed to achieve the medium. This simplifies the process and thus save the operational cost significantly. Another significant difference is the average particle density of the feed, which is about 1400 kg/m^3 for DMCs but about 1800 kg/m^3 for NMCs. These differences may require significantly changes for the design, control and optimization of NMCs when compared to that of DMCs.

A typical NMC technology is the Natural Medium Dual Density system developed by RecyCoal UK. The system has been successfully used at a number of sites in the UK and is now increasingly used worldwide including Australia. NMCs are the decisive devices in the system since they are actually responsible for the separation of coal product from rejects. RecyCoal has designed and installed the systems to process tonnages ranging from 300 tph up

to 2000 tph and coal yields ranging from as low as 4% to over 60% for recovering coal from various difficult "waste" materials such as:

- Old derelict colliery spoil tips
- Heat affected coal
- Rejects from dense medium cyclones
- Clay contaminated coal seams
- Coal from seam cleanings and interfaces
- Run-of mine feed direct from the mine.

Currently there is almost no experimental work on NMC in the literature. In fact, even for the traditional DMCs, the useful data for process design and control are limited because of the difficulty in conducting controlled experiments. To date, majority of the previous studies are limited to the quantification of macroscopic parameters (see [1] for example). A recent study has indicated that the measurement errors of separation performance Ep (Ep = $(D_{75}-D_{25})/2$, where D_{75} and D_{25} are the densities for which 75% and 25% of feed particles report to underflow respectively) of a large scale DMC (the mass flowrate is about 2000 tonnage per hour) is about 20% on average [2]. The major reason for this large measurement error should be that the properties of the coal particles such as coal particle size and density distributions are almost impossible to be the same for different runs of physical experiments while previous work has shown that the coal properties can significantly affect the cyclone performance [3-5]. Moreover, it is very difficult to measure the microscopic, internal flow and force structures in DMC/NMC. With the use of expensive techniques such as X-ray and gamma ray tomography, only the density distribution of medium flow (coal is not included) could be measured [6, 7].

Mathematical modelling, often supported by physical modelling, offers an alternative to understand the complicate phenomena in a NMC. Nonetheless, the modelling work on the

multiphase flows in DMC/NMC has been extremely challenging. The current models on DMCs could be generally divided into three catalogues: (i) the combined CFD and LPT (Lagrangian particle tracking) model in which the medium flow is modelled by CFD while the coal particles are tracked by LPT [8-13]; (ii) the CFD/Mixture model approach in which both medium and solids are treated as a kind of fluid and modelled by the Mixture model which can be regarded as a simplified two fluid model (TFM) [14]; and (iii) the CFD-DEM approach in which medium flow is modelled by CFD while solids are modelled by DEM which applies Newton's second laws to individual particles [4, 15, 16].

The CFD-LPT approach is able to qualitatively study the effect of parameters such as geometry, fluid flow velocity and particle size. However, it cannot satisfactorily describe the effect of solids on medium flow and consequently parameters such as solid concentration. In theory the calculation of the reaction force on fluid phase acted by solid phase is mainly based on solid concentration and the relative velocity between solids and fliud; the accurate prediction of solid concentration depends on the modelling of particle-particle interactions that is not usually shown in the LPT models [17]. In order overcome the deficiency of CFD-LPT model, various approaches have been developed to model parcel-parcel interactions in the CFD-LPT model framework [e.g., 18, 19].

The TFM model has been widely used in the literature for process modelling and especially for the modelling of fluidized beds [20-23]. However, it is extremely hard to apply a TFM to DMCs as there are particles of different densities and sizes (in theory particle of each density and size should be treated as a separate phase in the TFM model). So far, only a simplified TFM, i.e., the Mixture model has been attempted to study DMCs [14].

The CFD-DEM model has been proved to be an effective model to study the fundamentals of particle-fluid systems and has been extensively used in the literature in recent years [24, 25].

CFD-DEM has also been applied to model complicated particle-fluid flow systems including cyclones of different types [4, 5, 15, 16, 26]. Notably, in order to overcome the problem of high computational cost of a standard CFD-DEM model, CFD-DEM models with different treatments such as parcel-particle concept, coarse-graining (CG) model, similar particle assembly model or scaling laws have been developed for various particulate systems [5, 26-33].

In this work, a CG CFD-DEM model is developed to model the swirling multiphase flow in a NMC. The results are first evaluated against experimental data and then the effect of two of the most important operational parameters, i.e., medium velocity and medium-to-coal (M:C) ratio at the NMC inlet, is investigated numerically. It demonstrates that the developed model could be a useful tool to design, control and optimise NMCs.

2 MATHMATICAL MODEL

The CFD-DEM model used for the present work has been well documented in the literature [34-36]. Following the model strategy used for dense medium cyclones [4, 12, 16], the modelling was divided into three steps, as shown in Fig. 1. The first two steps are devoted to solving the medium slurry flow and the third step is the particle flow. The continuum medium flow is calculated from the continuity and the Navier-Stokes equations based on the local mean variables defined over a computational cell. These are given by

$$\frac{\partial(\rho_f \varepsilon)}{\partial t} + \nabla \cdot (\rho_f \varepsilon \mathbf{u}) = 0 \tag{1}$$

and

$$\frac{\partial(\rho_f \varepsilon \mathbf{u})}{\partial t} + \nabla \cdot (\rho_f \varepsilon \mathbf{u} \otimes \mathbf{u}) = -\nabla P - \mathbf{F}_{f-p} + \nabla \cdot (\varepsilon \boldsymbol{\tau}) + \rho_f \varepsilon \mathbf{g} + \nabla \cdot (-\rho_f \overline{\mathbf{u}' \otimes \mathbf{u}'}) \tag{2}$$

where ε, $\mathbf{u}$, $\mathbf{u}'$, t, ρ_f, P, $\mathbf{F}_{f\text{-}p}$, $\boldsymbol{\tau}$, and $\boldsymbol{g}$ are, respectively, porosity, mean and fluctuating fluid velocities, time, fluid density, static pressure, volumetric fluid-particle interaction force, fluid viscous stress tensor, and acceleration due to gravity. $\mathbf{F}_{f-p} = \frac{1}{V_{cell}} \sum_{i=1}^{k_c} \mathbf{f}_{p-f,i}$, where $\mathbf{f}_{p-f,i}$ is the total fluid force on particle i and k_c is the number of particles in a CFD cell of volume V_{cell}. $-\rho_f \overline{\mathbf{u}' \otimes \mathbf{u}'}$ is the Reynolds stress term due to turbulence and modelled by the Reynolds Stress Model (RSM) [37-41], while turbulence modification due to the presence of particles is not considered in this work.

The flow patterns derived by solving Eqs. (1) and (2) represent the mixture flow of medium and air. According to the work of Wang et al. [12, 42], the CFD modelling of medium and air flow was divided into two steps, as shown in Fig. 1. In step 1, only air and slurry are considered. The turbulence is modelled using the RSM, and the Volume of Fluid (VOF) model is used to describe the interface between the medium and the air core. In VOF, the two phases are considered immiscible and modelled by solving a single set of momentum equations and tracking the volume fraction of each of the fluids throughout the domain. The viscosity and density are the volume fraction weighted sum of the slurry and air values. At this stage, the position of the air core and the initial velocity distribution is obtained. The method is similar to that used for modelling multiphase flow in hydrocyclones [42]. In step 2, six additional phases are introduced to describe the behaviour of nature medium particles with different sizes. The multiphase model is changed from the VOF to the Mixture model where air phase is treated as one of the secondary phases. A model is also introduced to account for viscosity variation as a function of the volume fraction of nature medium particle [43]. Detailed density and velocity distributions of different phases are obtained at the end of this step. The details of the calculation of medium flow can be found elsewhere [12, 42].

In the third step, as shown in Fig. 1, the flow of coal particles are determined from the fluid flow patterns obtained above using either the Lagrangian Particle Tracking (LPT) or the DEM method. In this work, DEM [44] is used. Thus a particle in a fluid has two types of motion: translational and rotational, both obeying Newton's second law of motion. During its movement, the particle may collide with its neighbouring particles or with the wall and interact with the surrounding fluid, through which momentum is exchanged. At any time t, the equations governing the translational and rotational motions of particle *i* in this multi-phase flow system are:

$$m_i \frac{d\mathbf{v}_i}{dt} = \mathbf{f}_{p-f,i} + \sum_{j=1}^{k_i} \left(\mathbf{f}_{c,ij} + \mathbf{f}_{d,ij} \right) + m_i \mathbf{g} \tag{3}$$

and

$$\boldsymbol{I}_i \frac{\mathrm{d}\boldsymbol{\omega}_i}{\mathrm{d}t} = \sum_{j=1}^{k_i} \left(\mathbf{T}_{ij} + \mathbf{M}_{ij} \right) \tag{4}$$

where m_i, I_i, $\mathbf{v}_i$ and $\boldsymbol{\omega}_i$ are, respectively, the mass, moment of inertia, translational and rotational velocities of particle i. The forces acting on solids are the fluid-solids interaction force, $\mathbf{f}_{p-f,i}$, inter-particle forces between particles i and j, which include the contact forces, $\mathbf{f}_{c,ij}$, and viscous damping forces, $\mathbf{f}_{d,ij}$, and the gravitational force, $m_i\mathbf{g}$. Torques, $\mathbf{T}_{ij}$, are generated by the tangential forces and $\mathbf{M}_{ij}$ is the rolling friction torque that is in opposition to the rotation of the ith particle. The particle-fluid interaction forces considered in this work are the viscous drag force and pressure gradient force. Trial simulations indicate that other particle-fluid forces, such as the virtual mass force and the lift force, could be ignored. The fluid properties used to calculate the particle-fluid interaction forces are those relating to the properties of the mixture phase which are calculated from the individual phases, i.e., water, air and nature medium particles of different sizes by the mixture model. For simplicity, the

lubrication effect on particle-particle interaction and particle dispersion due to turbulence is not considered. The equations used to calculate the forces are shown in Table 1 and can also be found in the literature [25, 34, 45, 46].

A conventional DEM model is computationally very expensive as Newton's second law must to applied to each particle [44]. As particle size becomes very small, the number of particles increases exponentially. To overcome this problem it is necessary to adopt the concept of "Coarse-graining" (CG) or "parcel-particle" used by Patankar and Joseph [47]. Similar concepts or treatments have been used by other researchers to simulate large particulate systems [18, 19, 48]. According to the concept, a group of real particles with the same properties (size and density in the current case) can be represented by one CG particle. At a given point in the fluid flow, the acceleration of the CG particle due to fluid forces is assumed to be the same as that of the group of real particles it represents. However, the acceleration due to inter-particle forces and particle-wall forces are calculated according to the properties of the CG particle. Fig. 2 shows the major concept and assumptions of the approach. The general idea is that particles of same properties such as size and density could be grouped into one CG particle and all of the particles in the group will have same translational and rotational movement in the considered system. In other words, a large number of real particles of same properties are represented by a small number of parcel/CG particles. Notably, the particle group shown in Fig. 2 (c) should not be treated as a parcel/CG/model particle because one CG particle could not contain particles of different sizes. This is because particles of different size normally behave quite differently from each other especially within fluid. It should also be noted that there must be enough number of CG particles to make the representation of real particles using CG particles statistically reasonable. The details of the CG CFD-DEM model used in current work can be found in [5, 26]. Note that there are various models which have been applied to

model the medium-coal multiphase flows in DMCs in the literature, as summarized in Table 4 [49].

The modelling of the solids flow by DEM is at the individual particle level, whilst the fluid flow by CFD is at the computational cell level. Their two-way coupling (fluid forces act on particles and particles react on fluid) is numerically achieved as follows. At each time step, DEM provides information, such as the positions and velocities of individual particles, for the evaluation of porosity and volumetric particle-fluid interaction force in a computational cell. CFD then uses these data to determine the fluid flow field, from which the particle-fluid interaction forces acting on individual particles are determined. Incorporation of the resulting forces into DEM produces information about the motion of individual particles for the next time step [34].

3 SIMULATION CONDITIONS

The working principle in a NMC is schematically shown in Fig. 3. The feed, which is a mixture of water, waste coal, fine dirty, clay and shale etc., enters tangentially near the top of the cylindrical section, thus forming a strong swirling flow. Centrifugal effect causes the refuse or high ash particles to move towards the outer wall of the cyclone, where the axial velocity points predominantly downward, and to discharge through the spigot. The lighter coal particles, driven by the pressure gradient force and radial fluid drag force [16], move towards the longitudinal axis of the cyclone, where there is usually an air core, and the predominant axial velocity points upward and the coal exits through the vortex finder. In practice, the NMC is not operated vertically; instead, it is operated at certain orientation angle (the orientation angle is defined as the angle between the NMC axis and horizontal plane, as shown in Fig. 3).

The geometric parameters and mesh of the NMCs are representatively shown in Fig. 4 (a) and (b) (Note that the detailed dimensions of the NMC are not given due to commercial reasons). Following the meshing strategy in our previous works on cyclones [5, 12, 16, 17, 42], the NMC is divided into 112,087 hexahedral cells for the CFD computation, which is slightly finer than those used in some of the previous studies [e. g., 5, 16]. Trial simulation suggested that finer mesh does not obviously affect the simulation results (the difference is within 5%). Note that larger number of meshes could give more accurate results. However, considering the extremely high computational cost in the modelling of nature medium cyclones by using CFD-DEM approach (typically one run of simulation lasts about 2 months on a single prevailing CPU), we have used relatively smaller number of meshes in this work. It is expected that the mesh number used in this work is acceptable at least for industrial problems. We also adopted relatively low quality meshes in the inlet of the cyclone (in the regions closing to the cylinder body) while we have used high quality meshes in the swirling flow regions of the cyclone. We have checked the flow filed and found that this treatment does not obviously distort the simulation results in that region.

The pressure at the two outlets (vortex finder and spigot) is set to one atmosphere (101.325kPa) while different vortex finder pressure may lead to significantly different flow pattern [50]. The NMC is operated horizontally, i.e., the orientation angle is 0 degree. For simplicity, all coal particles are assumed to be spherical. Particle density is normalized by dividing by water density and so-called as relative density (RD). The medium-to-coal ratio is the ratio of the mass flowrate of medium at the NMC inlet to that of the coal particles. The operational parameters used in the simulation are summarised in Table 3.

According to Fig. 1, the simulation process is divided into three steps. In Step 1, the flow of water-air flow is solved (with turbulence at the inlet specified by 3% turbulent intensity and

0.128 m hydraulic diameter) to get converged results and reach its macroscopically steady state that is defined as the state when the flow properties just fluctuate around their respective average values, not varying with time. In Step 2, the flow of a mixture of water, air, fine dirty particles is solved to get converged results and reach its macroscopically steady state. In Step 3, waste coal particles are injected into the cyclone continuously from the inlet. The number of particles injected in a given time is calculated so as to match the pre-set medium-to-coal ratio at the NMC inlet. In order to get the partition performance of coal particles (partition number is defined as the portion of particles of certain density reporting to underflow of the NMC), the information of coal particles exiting from the overflow is collected during the period of macroscopically steady flow state (after injecting the coal particles, the flow can reach another macroscopically steady state in about 15 seconds in this work while the total simulation time after injecting coal is about 40 seconds).

The simulations are all unsteady, with the medium flow solved by using Ansys Fluent. The used pressure-velocity coupling scheme is "SIMPLE". The used spatial discretization schemes for pressure, momentum, and volume fraction are "PRESTO", "Second Order Upwind" and "QUICK" respectively.

4 RESULTS AND DISCUSSION

4.1 Model Validation

The CFD-DEM model used in this work has been validated step by step against experimental measurements in our previous studies [5, 12, 16, 42]. As shown in Fig. 1, there are three steps in the whole simulation process, thus, the validation of these models are accomplished step by step as well. For Step 1, the model used to simulate the gas-liquid flow is similar to that in a hydrocyclone. Therefore, the experimental measurement for a hydrocyclone at a laboratory

scale by Hsieh [51] is used for the validation. A good agreement was observed between the simulated and measured results, as reported elsewhere [42]. For Step 2, there is limited experimental data for the velocity distribution of the medium phases. Only the medium density distribution measured by Subramanian using gamma-ray tomography [52] is available for comparison. As expected, it is found that the simulated results are close to those measured [12]. In Step 3, the simulated partition curves of coal particles for different size agree reasonably with the experimental measurements [5]. The CG CFD-DEM model is also compared to a conventional standard CFD-DEM model and it is found that the error caused by the CG concept is generally acceptable [26]. Fig. 5 shows there is quantitatively agreement between simulation results obtained from the CG CFD-DEM model and experimental measurement data [53] for current NMC.

4.2 Effect of medium inlet velocity

For given NMC geometry and the medium-to-coal ratio, medium inlet velocity largely represents the throughput of the NMC. The flow field of medium is also important since it largely decides the flow of coal particles. Fig. 6 shows that the simulated medium flows in the NMC without coal. It can be seen that the flow fields all qualitatively agree with the previous findings [12]. That is, the static pressure decreases radially from wall to centre (Fig. 6(a)), the medium density at the lower part is higher than that at the upper part (Fig. 6(b)), the tangential velocity increases from the outer wall to the center of the DMC with its peak value in the region close to the air core (Fig. 6(c)). The axial velocity is upward in the centre region and downward at the regions close to the outer all of the NMC (Fig. 6(d)). Quantitatively, the flow field is different when the inlet velocities are different. Fig. 6 shows that the pressure drop, tangential and axial velocities all increases with inlet velocity. The relationship between inlet velocity and pressure drop is also shown in Table 5. It can be seen that under current conditions, the

pressure drop is as high as 37 psi when the medium volumetric flowrate is 600m^3/hr. On the other hand, the pressure drop is only 3.34 or 7.18 psi when the medium flowrate is 180 and 264 m^3/hr respectively, which corresponds to operational head of 3.74 and 8.04 respectively. Since the commonly used operational head in DMCs is from 6 to 12, it is thought the current NMC should be operated with medium flowrate of 200-400 m^3/hr. Actually, it was found from the CFD-DEM simulations that the particle-particle and particle-wall interaction forces can be very high when the medium flowrate is 600 m^3/hr and a converged results could not be obtained under such high medium flowrate.

Fig. 7 shows the partition curves obtained for different medium inlet velocities. Generally, there are two kinds of phenomena shown in the figure: one is that under this range the partition performance is not so sensitive to medium flow rate or operational head; another one is that as the medium inlet velocity increases, there are slightly more particles reporting to the overflow instead of the underflow.

The phenomena shown in Fig. 7 could be explained by using the forces acting on the particles in the radial direction of the cyclone. In the current CFD-DEM model, the radial movement of particles in the cyclone is determined by the centrifugal effect and other two forces, i.e., the radial pressure gradient force and the radial drag force. The centrifugal effect could be thought as another force acting on the particles and its magnitude is about $m_p \frac{v_{p,t}^2}{r}$ (where m_p is the mass of a particle, $v_{p,t}$ is the magnitude of the tangential velocity of the particle, and r is the radial position of the particle relative to the center of the cyclone). On one hand, as the tangential velocity of the particle ($v_{p,t}$) is largely proportional to the medium inlet velocity, the centrifugal effect is thus largely proportional to the square of the medium inlet velocity. On the other hand, the pressure drop in the NMC is also largely proportional to the square of the

medium inlet velocity (as demonstrated by Table 6). This suggests that both the centrifugal force and the pressure gradient force are proportional to the square of medium inlet velocity but they are in reverse directions to each other. Therefore, the enhanced centrifugal effect due to the increase of medium inlet velocity could be significantly compromised by the increased pressure gradient force. At the same time, the radial velocity of the medium phase will increase with the increase of medium inlet velocity, which would drive more particles to flow through the vortex finder of the cyclone and make the partition curve slightly shift toward the right hand side in Fig. 7. The shifting is not so significant since the radial drag force is much smaller than the radial pressure gradient force for current system where particle sizes are quite large (0.5-40 mm) [16]. The phenomena shown in Fig. 7 may not be observed in gas and hydro-cyclones where the drag force rather than pressure gradient force is the dominant force for separation.

4.3 Effect of medium-to-coal ratio (M:C ratio)

Medium-to-coal ratio (M:C ratio) represents the productivity of NMCs and thus one of the most important operational parameter of NMCs/DMCs. Fig. 8 shows that the partition performance of the current NMC is very sensitive to M:C ratio. As the M:C ratio decreases or the solids feed rate increases for given constant flow of medium, the partition curve shifts to the right, which means that there are more particles reporting to the overflow. It can be seen from Fig. 8 that when M:C ratio is larger than 8, the NMC is performing well. However, when M:C ratio is less than 5, there are very few particles reporting to the underflow, which means that the NMC is not working properly and there is almost no separation of particles by density. One of the reason could be shown in Fig. 9 which shows that the particle-particle interaction is very strong in the regions of the cylinder body of the NMC when M:C ratio is low (= 4.2). This may also correspond to the phenomenon (the internal report from the University of Leeds)

that the viscosity will be quite high when the medium feed density is up to 1.4. Overall, this suggests that the current NMC should not be operated under a M:C ratio lower than 5 (Note that in a typical DMC the M:C ratio can be usually quite low (from 3 to 5), which also highlights the importance of using fine magnetite particles to form the medium). In order to address this problem and also meet the needs of industry to process different kinds of waste coal, we have developed new designs of NMCs which is better than the current design but the results are not intended to be included in this work.

5 CONCLUSIONS

In this work, a numerical approach of combined Computational Fluid Dynamics and Discrete Element Method (CFD-DEM)) has been developed to simulate the coal-medium flow in a Natural Medium Cyclone (NMC) for the recovery of waste coal. The simulated results are validated against experimental data and previous findings in the literature either qualitatively or quantitatively depending on the availability of data. The simulation results are also analysed in terms of medium flow fields and coal flow patterns, and particle-particle interaction force to better understand the flow characters in NMCs. Specifically, the main findings include:

- The general flow patterns of both medium phase and coal particles in NMCs are similar to that in DMCs.

- The operational pressure/head of the studied NMC increase significantly with medium inlet velocity. Under low inlet velocity, the partition performance is not so sensitive to inlet velocity (the major reason is that the enhanced centrifugal effect due to the increase of medium inlet velocity is significantly compromised by the increased pressure gradient force). However, under quite high inlet velocity, there are extremely

large particle-particle interaction in the cylinder body of the NMC, which leads to difficulty in obtaining converged simulation results.

- The performance of the current NMC is very sensitive to medium-to-coal ratio. As medium-to-coal ratio decreases, there are large portion of high density particles reporting to the overflow. When the medium-to-coal ratio is 4.2 (the normal range of medium-to-coal ratio for a DMC is 3-7), there are almost no separation of particles by density in the NMC. The reason could be that there are extremely large particle-particle interaction force in the cylinder body of the NMC when medium-to-coal ratio is low. The high particle-particle interaction force pushes particles to flow into the centre of the NMC where the particles are dragged upward toward the overflow due to the upward flow of medium in the centre region of the NMC.

- Like DMC, NMC is affected by many variables related to geometry, material properties and operational conditions. A systematic study is necessary to understand their effects for process design and control. The proposed models, supported by some physical experiments and plant tests, would be a way to achieve this goal.

ACKNOWLEDGEMENT

The authors are grateful to RecyCoal UK and the Australia Research Council (ARC) for the financial support of this work.

NOMENCLATURE

A sample volume or area, m^3 or m^2

c damping coefficient, dimensionless

d particle diameter, m

E Young's modulus, Pa, or energy of the system

$\mathbf{f}_c$ contact force, N

$\mathbf{f}_d$ damping force, N

$\mathbf{f}_{p-f}$ particle-fluid interaction force, N

$\mathbf{F}_{p-f}$ interaction forces between fluid and solids phases, equal to $\sum_{i=1}^{k_c} \mathbf{f}_{p-f,i} / \Delta V_c$, N/m^3

$\mathbf{g}$ gravity acceleration vector, 9.81 m/s^2

$\mathbf{G}$ gravity vector, N

H operational head, dimensionless

I moment of inertia of a particle, kg·m

k shape parameter for particle size distribution, dimensionless

k_c number of particles in a computational cell, dimensionless

k_i number of particles in contact with particle i, dimensionless

k_m number of collisions in a sampling time interval, dimensionless

m mass of a particle, kg

$\mathbf{n}$ unit vector in the normal direction of two contact spheres, dimensionless

n shape parameter for Rosin-Rammler distribution, dimensionless

N_p the number of real particles represented by a coarse grain, dimensionless

P pressure, Pa

ΔP pressure drop, Pa

r the radial position of a particle relatively to the centre of the cyclone, m

$\mathbf{R}$ radius vector (from particle centre to a contact point), m

R magnitude of $\mathbf{R}$, m

Re	Reynolds number, dimensionless
t	time, s
T	total sampling time, s
$\mathbf{T}$	driving friction torque, N·m
$\mathbf{u}$	fluid velocity vector, m/s
V	volume, m^3
$\mathbf{v}$	particle velocity vector, m/s
ΔV_c	volume of a computational cell, m^3

Greek letters

α	size ratio of CG/parcel/model particle to original particle
β	empirical coefficient defined in Table 3, dimensionless
σ_j	shape parameter for particle density distribution, dimensionless
$\boldsymbol{\delta}$	vector of the particle-particle or particle-wall overlap, m
δ	magnitude of $\boldsymbol{\delta}$, m
ε	porosity, dimensionless
μ	fluid viscosity, kg/m/s
μ_r	coefficient of rolling friction, m
μ_s	coefficient of sliding friction, dimensionless
ν	Poisson's ratio, dimensionless
ρ	density, kg/m^3
$\boldsymbol{\tau}$	viscous stress tensor, N/m^3
$\boldsymbol{\omega}$	angular velocity, rad/s
ω	magnitude of angular velocity, rad/s

$\hat{\omega}$ unit angular velocity

Subscripts

c contact

d damping

D drag

f fluid phase

ij between particle i and j

$i(j)$ corresponding to $i(j)th$ particle

m medium phase

max maximum

n in normal direction

p particle phase

pg pressure gradient

$p-f$ between particle and fluid

t in tangential direction

Superscripts

cg coarse-grained particle

0 original particle

REFERENCES

[1] S. Hu, B. Firth, A. Vince, G. Lees, Prediction of dense medium cyclone performance from large size density tracer test, Minerals Engineering, 14 (2001) 741-51.

[2] G. Sherritt, A. Meyers, A. Bennetts, J. Graham, Delineation of large diameter dense medium cyclone performance, Australia, ACARP Report: C17036 (2010).

[3] J. Chen, K. W. Chu, R. P. Zou, A. B. Yu, A. Vince, G. D. Barnett, et al., Systematic study of effect of particle size distribution in a dense medium cyclone by Johnson's S-B function, Minerals Engineering, 91 (2016) 16-33.

[4] K. W. Chu, B. Wang, A. Vince, A. B. Yu, Computational study of the multiphase flow in a dense medium cyclone: Effect of particle density, Chemical Engineering Science, 73 (2012) 123-39.

[5] K. W. Chu, B. Wang, A. B. Yu, A. Vince, G. D. Barnett, P. J. Barnett, CFD-DEM study of the effect of particle density distribution on the multiphase flow and performance of dense medium cyclone, Minerals Engineering, 22 (2009) 893-909.

[6] V. J. Subramanian, Measurement of medium segregation in the dense medium cyclone using gamma-ray tomography, PhD Thesis, University of Queensland, Australia (2002).

[7] K. P. Galvin, J. B. Smitham, Use of X-rays to determine the distribution of particles in an operating cyclone, Minerals Engineering, 7 (1994) 1269-80.

[8] M. Narasimha, M. S. Brennan, P. N. Holtham, T. J. Napier-Munn, A comprehensive CFD model of dense medium cyclone performance, Minerals Engineering, 20 (2007) 414-26.

[9] M. Narasimha, M. S. Brennan, P. N. Holtham, Numerical simulation of magnetite segregation in a dense medium cyclone, Minerals Engineering, 19 (2006) 1034-47.

[10] B. Wang, K. W. Chu, A. B. Yu, A. Vince, Computational investigation of the mechanisms of the “breakaway” effect in a dense medium cyclone, Minerals Engineering, 62 (2014) 111-9.

[11] B. Wang, K. W. Chu, A. B. Yu, A. Vince, G. D. Barnett, P. J. Barnett, Computational study of the multiphase flow and performance of dense medium cyclones: Effect of body dimensions, Minerals Engineering, 24 (2011) 19-34.

[12] B. Wang, K. W. Chu, A. B. Yu, A. Vince, Modeling the multiphase flow in a dense medium cyclone, Industrial & Engineering Chemistry Research, 48 (2009) 3628-39.

[13] B. Wang, K. W. Chu, A. B. Yu, A. Vince, Numerical studies of the effects of medium properties in dense medium cyclone operations, Minerals Engineering, 22 (2009) 931-43.

[14] S. B. Kuang, Z. Qi, A. B. Yu, A. Vince, G. D. Barnett, P. J. Barnett, CFD modeling and analysis of the multiphase flow and performance of dense medium cyclones, Minerals Engineering, 62 (2014) 43-54.

[15] K. W. Chu, S. B. Kuang, A. B. Yu, A. Vince, G. D. Barnett, P. J. Barnett, Prediction of wear and its effect on the multiphase flow and separation performance of dense medium cyclone, Minerals Engineering, 56 (2014) 91-101.

[16] K. W. Chu, B. Wang, A. B. Yu, A. Vince, CFD-DEM modelling of multiphase flow in dense medium cyclones, Powder Technology, 193 (2009) 235-47.

[17] K. W. Chu, B. Wang, A. B. Yu, D. L. Xu, Y. X. Chen, CFD-DEM simulation of the gas-solid flow in a cyclone separator, Chemical Engineering Science, 66 (2011) 834-47.

[18] N. Huber, M. Sommerfeld, Modelling and numerical calculation of dilute-phase pneumatic conveying in pipe systems, Powder Technology, 99 (1998) 90-101.

[19] Y. Tsuji, T. Tanaka, S. Yonemura, Cluster patterns in circulating fluidized beds predicted by numerical simulation (discrete particle model versus two-fluid model), Powder Technology, 95 (1998) 254-64.

[20] D. Gidaspow, Multiphase Flow and Fluidization, Academic Press, (1994).

[21] J. L. Sinclair, R. Jackson, Gas-particle flow in a vertical pipe with particle-particle interactions, AIChE Journal, 35 (1989) 1473-86.

[22] T. B. Anderson, R. Jackson, A fluid mechanical description of fluidized beds, Industrial & Engineering Chemistry Fundamentals, 6 (1967) 527-39.

[23] J. Wang, M. A. van der Hoef, J. A. M. Kuipers, The role of scale resolution versus inter-particle cohesive forces in two-fluid modeling of bubbling fluidization of Geldart A particles, Chemical Engineering Science, 66 (2011) 4229-40.

[24] H. P. Zhu, Z. Y. Zhou, R. Y. Yang, A. B. Yu, Discrete particle simulation of particulate systems: A review of major applications and findings, Chemical Engineering Science, 63 (2008) 5728-70.

[25] H. P. Zhu, Z. Y. Zhou, R. Y. Yang, A. B. Yu, Discrete particle simulation of particulate systems: Theoretical developments, Chemical Engineering Science, 62 (2007) 3378-96.

[26] K. Chu, J. Chen, A. Yu, Applicability of a coarse-grained CFD–DEM model on dense medium cyclone, Minerals Engineering, 90 (2016) 43-54.

[27] M. Sakai, M. Abe, Y. Shigeto, S. Mizutani, H. Takahashi, A. Viré, et al., Verification and validation of a coarse grain model of the DEM in a bubbling fluidized bed, Chem Eng J, 244 (2014) 33-43.

[28] M. A. Mokhtar, K. Kuwagi, T. Takami, H. Hirano, M. Horio, Validation of the similar particle assembly (SPA) model for the fluidization of Geldart's group A and D particles, AIChE Journal, 58 (2012) 87-98.

[29] H. Kruggel-Emden, F. Stepanek, A. Munjiza, A study on adjusted contact force laws for accelerated large scale discrete element simulations, Particuology, 8 (2010) 161-75.

[30] S. Benyahia, J. E. Galvin, Estimation of Numerical Errors Related to Some Basic Assumptions in Discrete Particle Methods, Industrial & Engineering Chemistry Research, 49 (2010) 10588-605.

[31] M. Sakai, S. Koshizuka, Large-scale discrete element modeling in pneumatic conveying, Chemical Engineering Science, 64 (2009) 533-9.

[32] C. Bierwisch, T. Kraft, H. Riedel, M. Moseler, Three-dimensional discrete element models for the granular statics and dynamics of powders in cavity filling, J Mech Phys Solids, 57 (2009) 10-31.

[33] S. C. Thakur, J. Y. Ooi, H. Ahmadian, Scaling of Discrete element model parameters for cohesionless and cohesive solid, Powder Technology, 293 (2015) 130-7.

[34] B. H. Xu, A. B. Yu, Numerical simulation of the gas-solid flow in a fluidized bed by combining discrete particle method with computational fluid dynamics, Chemical Engineering Science, 52 (1997) 2785-809.

[35] Y. Tsuji, T. Kawaguchi, T. Tanaka, Discrete particle simulation of 2-dimensional fluidized-bed, Powder Technology, 77 (1993) 79-87.

[36] Z. Y. Zhou, S. B. Kuang, K. W. Chu, A. B. Yu, Discrete particle simulation of particle-fluid flow: model formulations and their applicability, Journal of Fluid Mechanics, 661 (2010) 482-510.

[37] F. S. Lien, M. A. Leschziner, Assessment of turbulence-transport models including nonlinear RNG eddy-viscosity formulation and 2nd-moment closure for flow over a backward-facing step, Computers & Fluids, 23 (1994) 983-1004.

[38] B. E. Launder, Second-moment closure and its use in modelling turbulent industrial flows, International Journal for Numerical Methods in Fluids, 9 (1989) 963-85.

[39] M. M. Gibson, B. E. Launder, Ground effects on pressure fluctuations in the atmospheric boundary layer, Journal of Fluid Mechanics, 86 (1978) 491-511.

[40] B. E. Launder, G. J. Reece, W. Rodi, Progress in the development of a Reynolds-stress turbulence closure, Journal of Fluid Mechanics, 68 (1975) 537-66.

[41] B. J. Daly, F. H. Harlow, Transport equations in turbulence, Phys Fluids, 13 (1970) 2634-49.

[42] B. Wang, K. W. Chu, A. B. Yu, Numerical study of particle-fluid flow in a hydrocyclone, Industrial & Engineering Chemistry Research, 46 (2007) 4695-705.

[43] M. Ishii, K. Mishima, Two-fluid model and hydrodynamic constitutive relations, Nuclear Engineering and Design, 82 (1984) 107-26.

[44] P. A. Cundall, O. D. L. Strack, Discrete numerical-model for granular assemblies, Geotechnique, 29 (1979) 47-65.

[45] L. W. Rong, K. J. Dong, A. B. Yu, Lattice-Boltzmann simulation of fluid flow through packed beds of uniform spheres: Effect of porosity, Chemical Engineering Science, 99 (2013) 44-58.

[46] Y. C. Zhou, B. D. Wright, R. Y. Yang, B. H. Xu, A. B. Yu, Rolling friction in the dynamic simulation of sandpile formation, Physica a-Statistical Mechanics and Its Applications, 269 (1999) 536-53.

[47] N. A. Patankar, D. D. Joseph, Modeling and numerical simulation of particulate flows by the Eulerian-Lagrangian approach, International Journal of Multiphase Flow, 27 (2001) 1659-84.

[48] M. Sakai, T. Yamamoto, M. Murazaki, Y. Miyoshi, Effect of particulate behavior on criticality evaluation in agitating powder of nuclear fuel, Powder Technology, 148 (2004) 67-71.

[49] K. W. Chu, B. Wang, A. Vince, A. B. Yu, Modelling the multiphase flow in dense medium cyclones, Journal of Computational Multiphase Flows, 2 (2010) 249-75.

[50] K. W. Chu, B. Wang, A. B. Yu, A. Vince, Particle scale modelling of the multiphase flow in a dense medium cyclone: Effect of vortex finder outlet pressure, Minerals Engineering, 31 (2012) 46-58.

[51] K. T. Hsieh, Phenomenological model of the hydrocyclone, PhD Thesis, The University of Utah, USA (1988).

[52] V. J. Subramanian, Measurement of medium segregation in the dense medium cyclone using gamma-ray tomography, Ph.D Thesis, University of Queensland, 2002).

[53] RecyCoal Ltd. internal report, (2011).

List of tables

List of figures

Table 1 Comparison of DMC and NMC technology.

Aspects	DMC	NMC
Medium type	Fine magnetite particles added into the feed	The fine dirt, shale and clay within the feed
Feed	Run-of-mine coal particles with average density of about 1400 kg/m^3	Mainly the rejects from DMC with particles average density of about 1800 kg/m^3
Product	Coal	The product of a NMC is usually then fed into a DMC again to get high quality coal product
Body geometry	With relatively long cylinder and cone parts	With relatively short cylinder and cone parts

Table 2 Equations used to calculate the forces and torques acting on particle i.

Forces and torques		Symbols	Equations
Normal forces	Contact	$\mathbf{f}_{cn,ij}$	$-\frac{E}{3\left(1-\nu^2\right)}\sqrt{2R_i}\delta_n^{3/2}\mathbf{n}$
	Damping	$\mathbf{f}_{dn,ij}$	$-c_n\left(\frac{3m_iE}{\sqrt{2}\left(1-\nu^2\right)}\sqrt{R\delta_n}\right)^{1/2}\mathbf{v}_{n,ij}$
Tangential forces	Contact	$\mathbf{f}_{ct,ij}$	$-\frac{\mu_s\mathbf{f}_{cn,ij}}{\lvert\delta_t\rvert}\left[1-\left(1-\frac{\min\left\{\lvert\delta_t\rvert,\ \delta_{t,\max}\right\}}{\delta_{t,\max}}\right)^{3/2}\right]\delta_t$
	Damping	$\mathbf{f}_{dt,ij}$	$-c_t\left(6m_i\mu_s\mathbf{f}_{cn,ij}\frac{\sqrt{1-\delta_t/\delta_{t,\max}}}{\delta_{t,\max}}\right)^{1/2}\mathbf{v}_{t,ij}$
Torque	Rolling	$\boldsymbol{T}_{ij}$	$\mathbf{R}_i\times\left(\mathbf{f}_{ct,ij}+\mathbf{f}_{dt,ij}\right)$
	Friction	$\boldsymbol{M}_{ij}$	$-\mu_r\mathbf{f}_{cn,ij}\hat{\boldsymbol{\omega}}_i$
Body force	Gravity	$\mathbf{G}_i$	$m_i\mathbf{g}$
Particle-fluid interaction force	Viscous drag force	$\mathbf{f}_{d,i}$	$\left(0.63+\frac{4.8}{\mathrm{Re}_{p,i}^{0.5}}\right)^2\frac{\rho_f\lvert\mathbf{u}_i-\mathbf{v}_i\rvert\left(\mathbf{u}_i-\mathbf{v}_i\right)}{2}\frac{\pi d_i^2}{4}\varepsilon_i^{-\beta}$
	Pressure gradient force	$\mathbf{f}_{pg,i}$	$V_{p,i}\nabla P$

where: $\boldsymbol{n}=\frac{\boldsymbol{R}_i}{R_i}$, $\mathbf{v}_{ij}=\mathbf{v}_j-\mathbf{v}_i+\omega_j\times\mathbf{R}_j-\omega_i\times\mathbf{R}_i$, $\mathbf{v}_{n,ij}=\left(\mathbf{v}_{ij}\bullet\mathbf{n}\right)\bullet\mathbf{n}$,

$$\mathbf{v}_{t,ij}=\left(\mathbf{v}_{ij}\times\mathbf{n}\right)\times\mathbf{n},\quad \hat{\omega}_i=\frac{\boldsymbol{\omega}_i}{\omega_i},\quad \mathrm{Re}_{p,i}=\frac{d_i\rho_f\varepsilon_i\lvert\mathbf{u}_i-\mathbf{v}_i\rvert}{\mu_f},$$

$$\beta=2.65(\varepsilon+1)-(5.3-3.5\varepsilon)\varepsilon^2\exp\left[-\frac{\left(1.5-\log\mathrm{Re}_{p,i}\right)^2}{2}\right],\quad \varepsilon=1-\frac{\sum_{i=1}^{k_{cell}}\boldsymbol{V}_i}{\Delta\boldsymbol{V}_{cell}}$$

Table 3 Operational conditions and material properties considered in the simulations.

Phase	Parameter	Symbol	Units	Value
Solid[a]	Density	ρ	Kg/m^3	1200 to 2200 with average density of 1800 (contain around 10% coal)
	Particle diameter	d_i	mm	0.5-40 (Rosin-Rammler) with average size of 5
	Rolling friction coefficient	μ_r	mm	0.005
	Sliding friction coefficient	μ_s	--	0.3
	Poisson's ratio	ν	--	0.3
	Young's modulus	E	N/m^2	1×10^7
	Damping coefficient	c	--	0.3
	Particle velocity at inlet	--	m/s	3.8
	Time step	--	s	2×10^{-5}
Gas	Density	ρ	kg/m^3	1.225
	Viscosity	μ	kg/m/s	1.8×10^{-5}
	Velocity at inlet	--	m/s	3.9
Water	Density	ρ	kg/m^3	998.2
	Viscosity	μ	kg/m/s	0.001
	Velocity at inlet	--	m/s	3-10
Nature medium particle	Density	ρ	kg/m^3	2500
	Sizes (volume fractions in slurry)	--	μm	2 (4.0%), 7 (3.4%), 15 (1.9%), 32 (1.5%), 54 (1.3%) and 82 (1.1%)
Medium phase[b]	Viscosity	μ	kg/m/s	Ishii and Mishima [43]
	Density	ρ	kg/m^3	1,250
	Velocity at inlet	--	m/s	3; 4.4; 5; 10;
	Time step	--	s	0.0025

[a] For convenience, the wall is assumed to be smooth and have the same properties as particles but infinite diameter.
[b] Standard wall function in Ansys Fluent is applied.

Table 4. Comparison of different models used in the modelling of the coal-particle flow in DMCs.

Model	Assumptions	Features
CFD-LPT	Neglect particle-particle interaction and the reaction of particles on fluid. Only limited number of particles is tracked.	$\mathbf{F}_{pf} = 0$ in Equ. (2). $\left(\mathbf{f}_{c,ij} + \mathbf{f}_{d,ij}\right) = 0$ in Equ. (3). Equ. (4) is not solved.
CFD-DEM one-way coupling	Neglect the reaction of particles on fluid.	$\mathbf{F}_{pf} = 0$ in Equ. (2).
CFD-DEM two-way coupling with CG concept	Use large "coarse-grained (CG)" particles to represent small particles. The material properties of the CG particles to calculate particle-particle and particle-wall interaction forces is assumed to be as same as that of the real particle or determined empirically.	$\left(\mathbf{f}_{c,ij} + \mathbf{f}_{d,ij}\right)$ in Equ. (3) and $\left(\mathbf{T}_{c,ij} + \mathbf{T}_{r,ij}\right)$ in Equ. (4) may not be realistic.
CFD-DEM two-way coupling	Least assumptions when compared with the other three models above.	Equs. (1-4) are all solved.

Table 5. The relationship between the medium flowrate and pressure or the effect of medium inlet velocity.

Medium flowrate (m^3/h)	Inlet velocity (Vin, m/s)	Pressure drop (Pa)	Pressure (psi)	Head
180	3	23000.00	3.34	3.74
264	4.4	49475.56	7.18	8.04
300	5	63888.89	9.27	10.38
600	10	255555.56	37.07	41.53

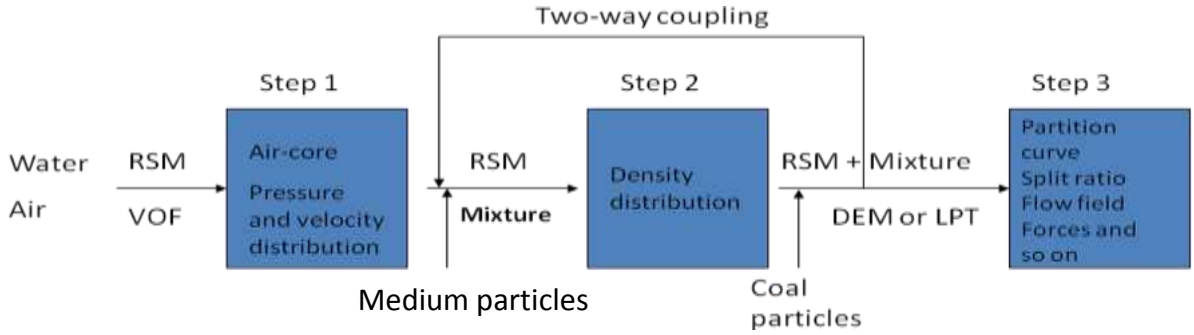

Fig. 1 Model strategy used in this work.

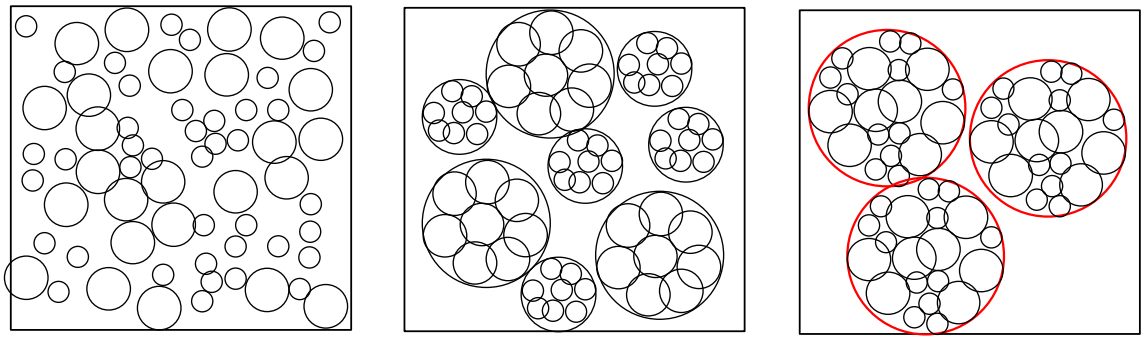

(a) (b) (c)

Fig. 2. Schematic representation of the main concept of the CG CFD-DEM model in a computational cell (there are particles of two sizes in each of the systems). (a), the original system; (b), a parcel/Coarse-grained system; (c), an example of inappropriate/wrong coarse-graining scheme (one CG particle can NOT contain particles of different sizes) [26].

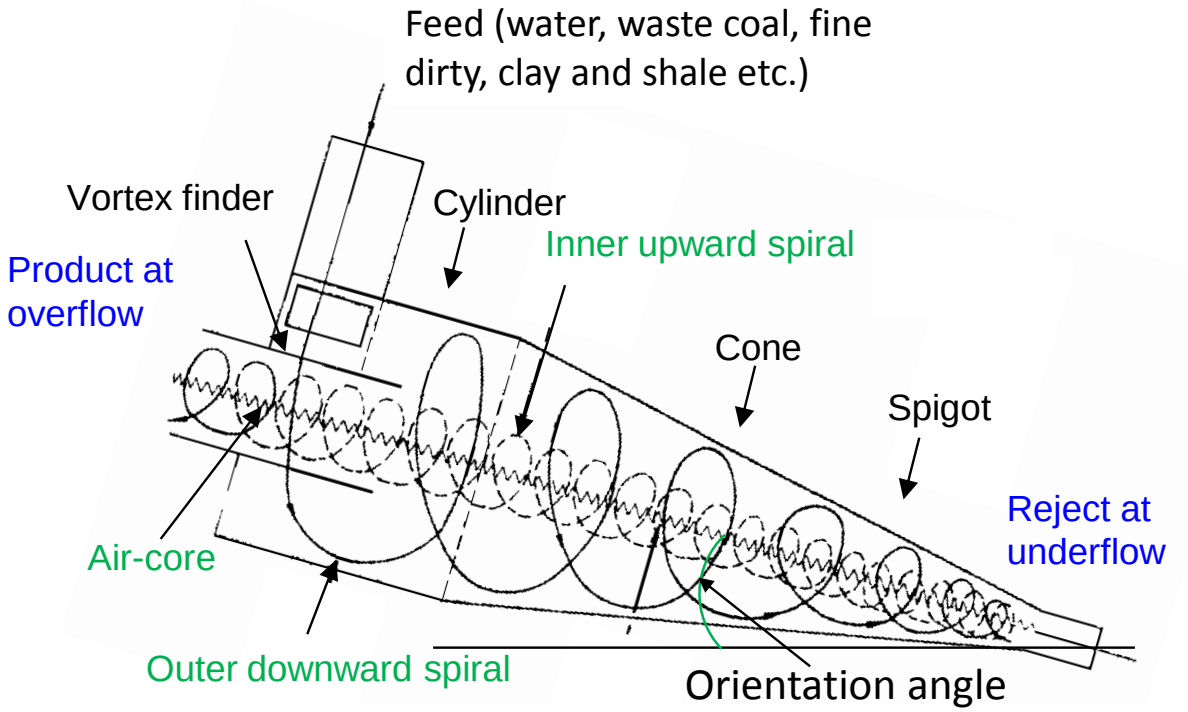

Fig. 3. A schematic presentation of a DMC/NMC operated in coal industry [26].

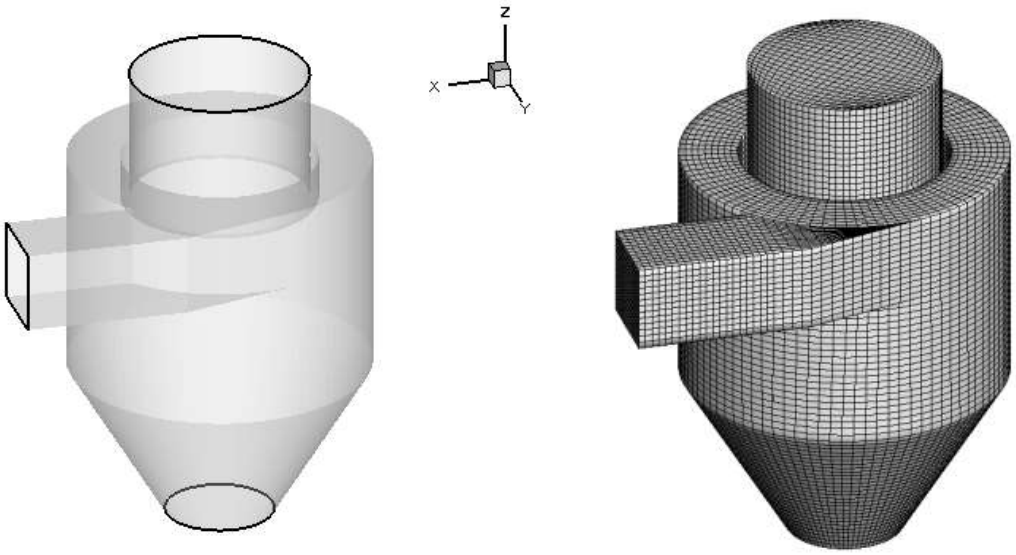

(a) (b)

Fig. 4. Representative presentation of the geometry (a) and mesh (b) of the simulated NMCs (Note that due to commertial reasons the detailed dimensions of the NMC are not allowed to be disclosed).

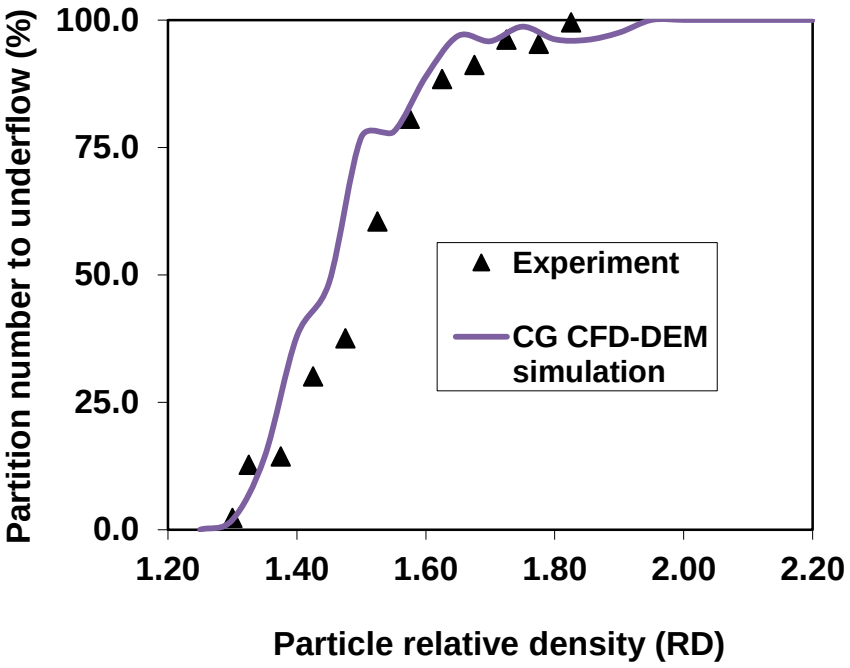

Fig. 5. Comparison of the simulated and measured partition curves (medium inlet velocity is 4.4 m/s and the NMC has a tangential inlet).

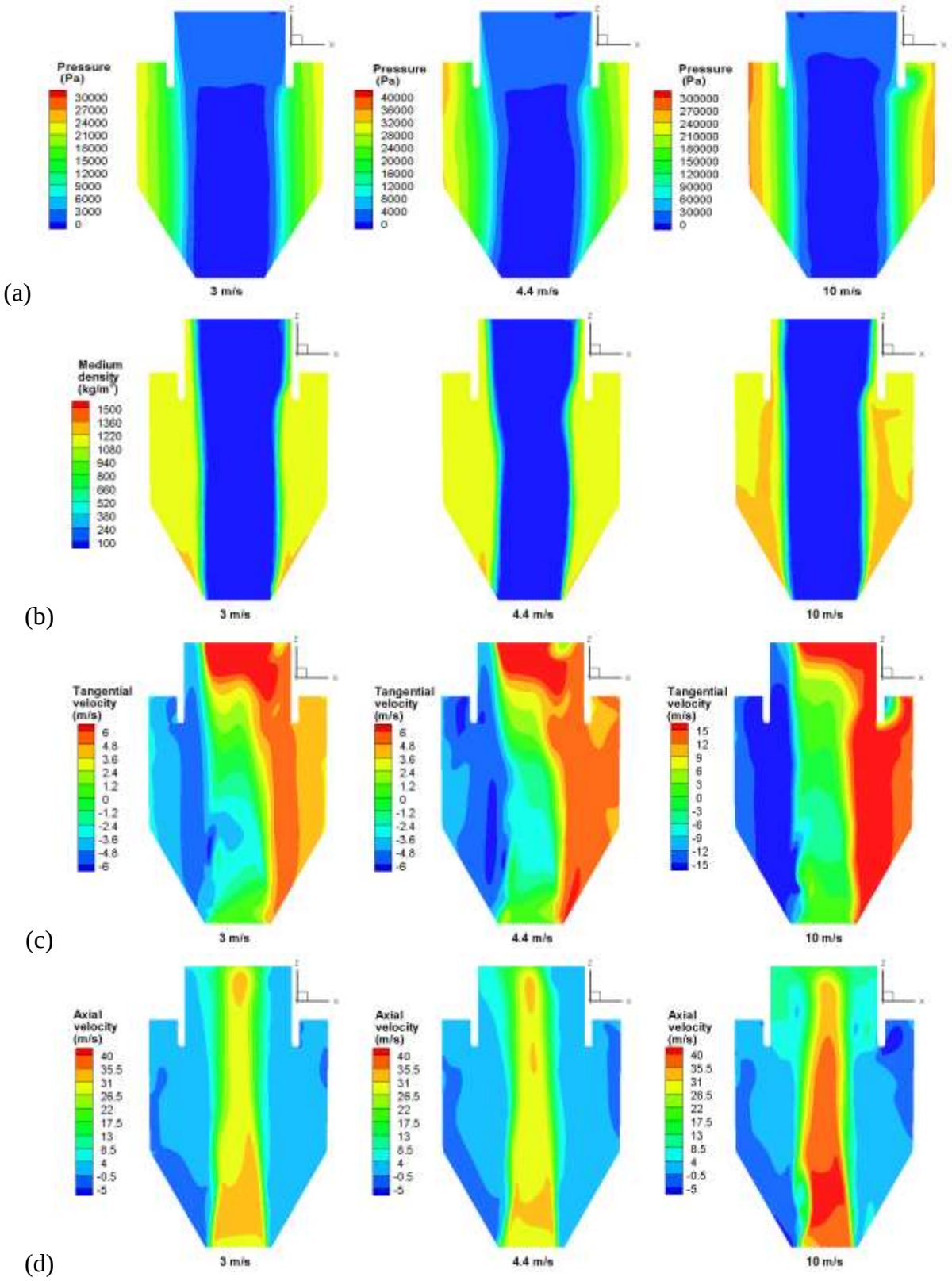

Fig. 6. Simulated medium flow field with tangential inlet for different medium inlet velocities. (a) Static pressure; (b) density distribution; (c) tangential velocity; and (d) axial velocity.

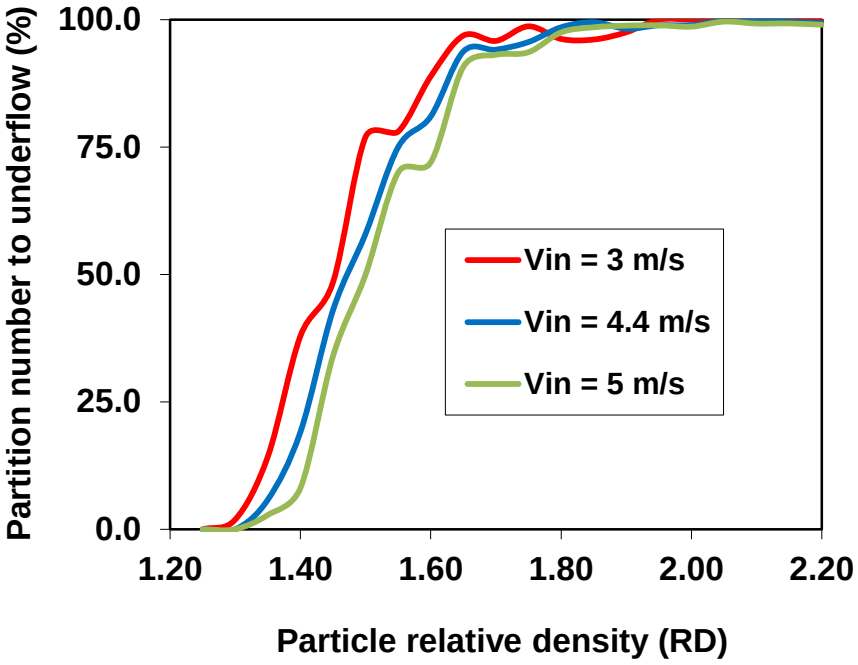

Fig. 7. Simulated and partition curves for different medium velocity at inlet when medium-to-coal ratio is 10 (for high velocity of 10m/s, a converged solution of CFD-DEM simulations has not been obtained).

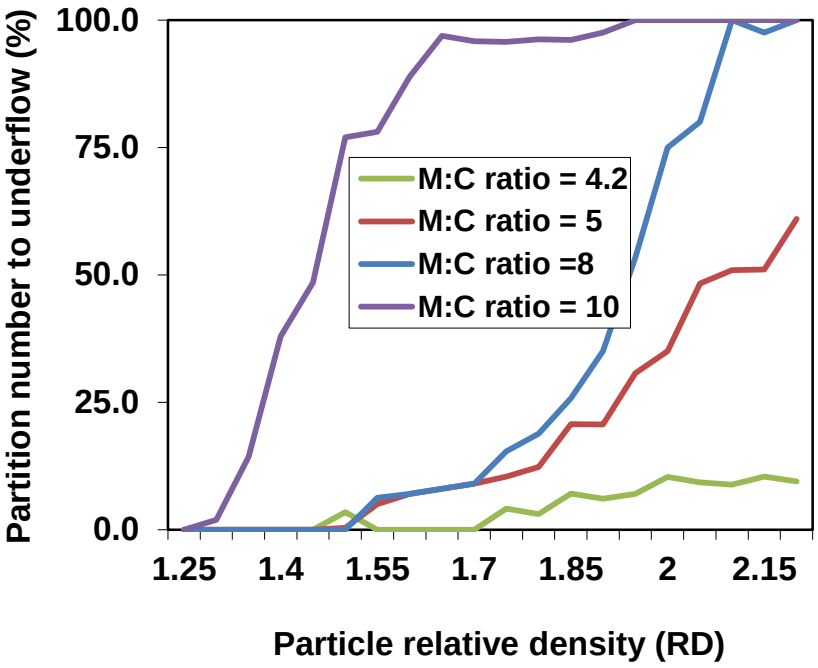

Fig. 8. Comparison of simulated and measure partition curves under different M:C ratio conditions.

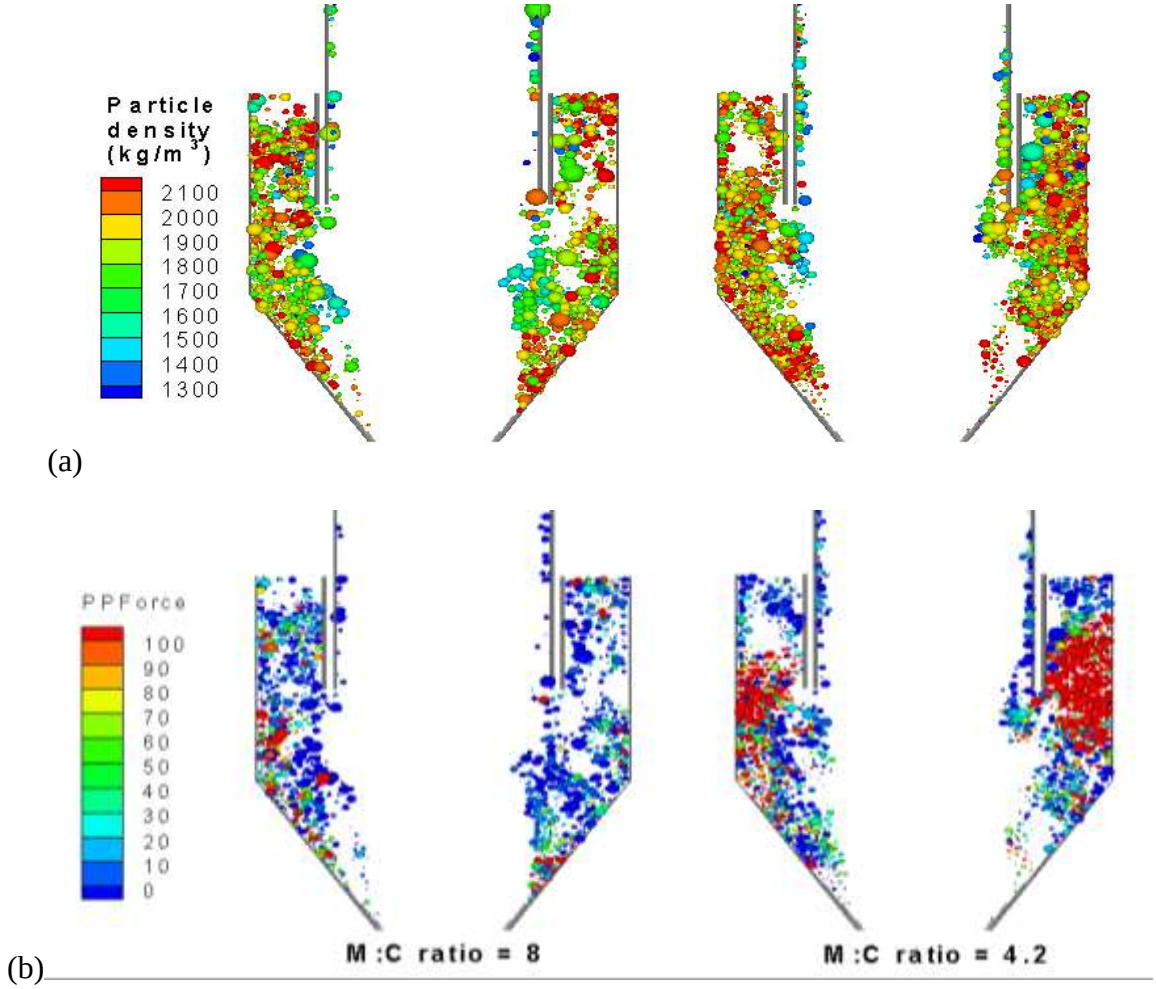

Fig. 9. Comparison of simulated spatial distributions of particles (a) and particle-particle interaction force (b) under different M:C ratios (the force is normalized by dividing by particle gravity).

Graphic abstract

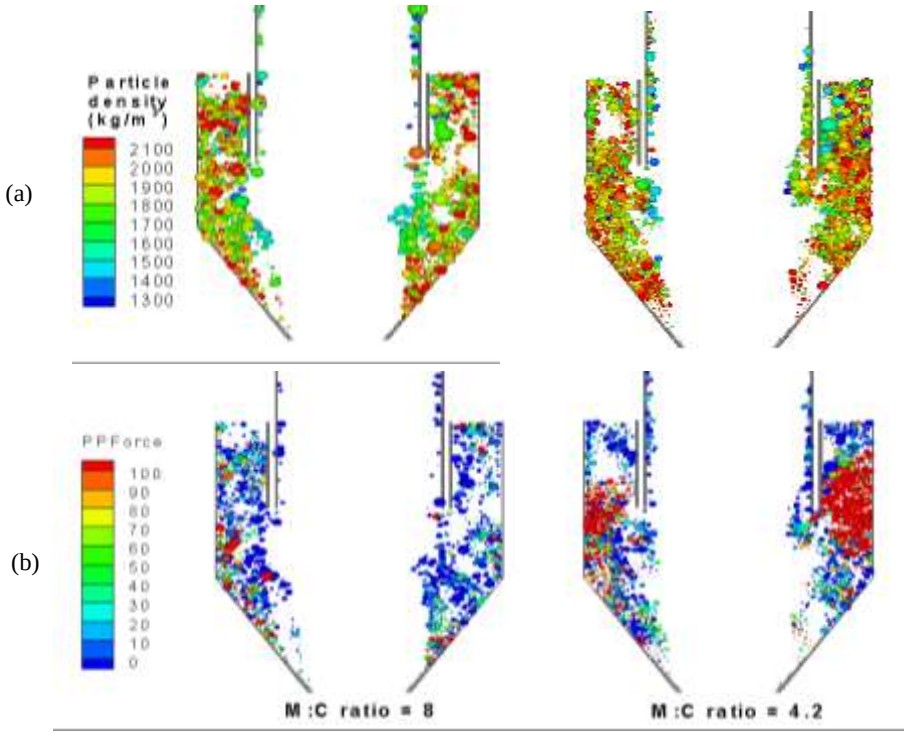

This figure shows the comparison of simulated spatial distributions of particle (a) and particle-particle interaction force (the force is normalized by dividing by particle gravity) (b) under different medium-to-coal (M:C) ratios. There are excessive large particle-particle interaction force regions in the cylinder body of the NMC when the M:C ratio is low, which causes large portion of high density particles reporting to the overflow.

Highlights

- A CFD-DEM model is developed to study nature medium cyclone
- The CFD-DEM results agree with experimental data
- The cyclone performance is not so sensitive to inlet velocity in current conditions
- The cyclone performance is very sensitive to medium-to-coal ratio